XMCD characterization of rare-earth dopants in $Ni_{81}Fe_{19}$(50nm): microscopic basis of engineered damping

W. E. Bailey, H. Song, and L. Cheng

Materials Science Program, Department of Applied Physics,

200 S.W. Mudd Bldg, Columbia University, New York, NY 10027

(Dated: February 2, 2008)

Abstract

We present direct evidence for the contribution of local orbital moments to the damping of magnetization precession in magnetic thin films. Using x-ray magnetic circular dichroism (XMCD) characterization of rare-earth (RE) $M_{4,5}$ edges in $Ni_{81}Fe_{19}$ doped with $< 2\%$ Gd and Tb, we show that the enhancement of GHz precessional relaxation is accompanied by a significant orbital moment fraction on the RE site. Tb impurities, which enhance the Landau-Lifshitz(-Gilbert) LL(-G) damping $\lambda(\alpha)$, show a spin to orbital number ratio of 1.5 ± 0.3; Gd impurities, which have no effect on damping, show a spin to orbital number ratio of zero within experimental error. The results indicate that the dopant-based control of magnetization damping in RE-doped ferromagnets is an atomistic effect, arising from spin-lattice coupling, and thus scalable to nanometer dimensions.

PACS numbers: 72.10.-d, 73.61.At, 75.70. -i , 75.70.Pa

INTRODUCTION

Ultrafast magnetization dynamics are important for determining the data rate (> 1GHz) of magnetic information storage.[1] Recent advances in time-domain measurement techniques have provided clear pictures of the ensemble[2, 3] and sub-micron spatial[4] response of magnetization to short magnetic field pulses, governed by the Landau-Lifshitz (LL) or -Gilbert (LLG) equations. The LL relaxation rate λ or Gilbert damping α determines the characteristic time for the magnetization to relax into new equilibria. Characteristic times are given by $2/\lambda$ (LL) or $2/\mu_o M_s \gamma \alpha$ (LLG) and are on the order of 2 ns in $Ni_{81}Fe_{19}$(50nm).

Dilute concentrations of rare-earth (RE(dopant atoms can be used to increase the damping of the precession in $Ni_{81}Fe_{19}$, speeding the return of magnetization to equilibrium.[5, 6] Terbium (Tb, 0-10%) has been shown to provide roughly two orders of magnitude of enhancement in α[5], from $0.006 \leq \alpha \leq 0.7$. The contributed damping has been found to be general for lanthanide dopants Sm-Ho, with effectiveness scaling roughly with the nominal orbital moment $< \hat{L_{RE}} >$ of the dopant $4f$ shell.[7]. Consistent with this idea, and with early measurements of FMR linewidth in RE-substituted YIG[8, 9], Gd dopants have shown no significant effect on damping.

Direct evidence has not been available previously to link RE impurity magnetization states to precessional damping, either in YIG or in modern thin-film magnetic systems. The rare earth magnetization is usually approximated as that of an isolated $4f$ shell, occupied as $4f^{Z-57}$, where Z is the atomic number of the RE impurity; spin, orbital, and total moments (S, L, J) are calcuated using Hund's rules. This approach yields moments which agree well with experimental moments except for metallic lanthanides near Eu[10]; measurement of the magnetic character of Gd and Tb in a metallic alloy is therefore worthwhile.

X-ray magnetic circular dichroism (XMCD) is an ideal tool to characterize the magnetic character of RE dopants. Orbital and spin moments $< L >$ and $< S >$ can be measured separately on individual atomic sites using sum rules[11, 12]. High resolution XMCD data have been measured previously in Tb single crystals at $M_{4,5}$ edges[13] and in Gd single crystals at the M_5 edge[14]. To our knowledge, however, sum rules have not yet been applied to the dilute RE impurities in transition metal ferromagnets relevant for controlled damping.

We have used XMCD to measure spin to orbital moment ratios of Gd and Tb (2%)

in $Ni_{81}Fe_{19}$(50nm). We show that for these elements, the calculated L/S ratios from a $4f^{Z-57}$ shell are verified. A fivefold enhancement in GHz relaxation rate from Tb dopants is accompanied by a large orbital moment fraction on the Tb site, indicating that spin-lattice coupling is decisive in enhancing relaxation.

EXPERIMENTAL

Films were deposited and magnetization dynamics were measured using methods described in ref. [7]. $Ni_{81}Fe_{19}$ (50 nm) thin films were prepared with 2% atomic concentrations of Gd and Tb. Films were deposited using ion beam deposition in a load-locked, multitarget chamber with base pressure of 6x10^{-8} Torr. Doping concentrations were measured as 1.7% of Gd and 1.8% of Tb using Rutherford Backscattering Spectroscopy (RBS). The top surface of the films was protected by a 20 Å Ta cap layer[24]

Magnetization dynamics of the thin films were characterized using time-domain pulsed inductive microwave magnetometry (PIMM). Measured waveforms are proportional to $\partial\phi/\partial t(t)$, where ϕ is the in-plane angle of the magnetization. A bias field H_B is applied along the magnetic (induced) easy-axis direction, orthogonal to the pulsed field; $H_B = 20$ Oe unless noted otherwise. See refs [3, 5] for details. Magnetization dynamics were measured within one day of deposition; samples were stored in a dessicator for less than a week before XMCD measurement.

XMCD measurements were taken in total electron yield mode (TEY) at the UV ring of the National Synchrotron Light Source (NSLS), Brookhaven National Laboratory, Beamline U4B.[15] XMCD was measured for fixed circular photon helicity, 75% polarization, with pulsed magnetization switching ($H = \pm 300$ Oe) at the sample; photon incidence was fixed at 45° with respect to the sample normal. The samples were mounted with magnetic easy axis along the applied field direction; measurements taken at remanence and in a saturating field were not found to differ appreciably. XMCD measurements with $H+$ ($M+$) measured first and $H-$ ($M-$) measured second were averaged with measurements taken in reversed order ("duplex mode"), to correct for any drift in the monochromator which might lead to derivative-like artifacts in XMCD. XMCD measurements were divided by the factor $0.75\cos 45°$ to correct for non-grazing incidence and incomplete circular polarization.

Sample TEY currents were normalized to TEY currents measured at a reference grid

(I_o), located ahead of the sample, to correct for any variation in beam intensity over the measurement. Photon energies could be varied continuously in the experiment from 500 - 1350 eV using a grating monochromator, with a general drop in beam intensity towards higher photon energies. High photon energies (1130-1320 eV) were calibrated using electron yield signals from inline Eu_2O_3 and Dy_2O_3 powder references, taking RE edge positions for the oxides reported in ref. [16]. A +3kV extraction voltage was applied near the sample surface; this was found to be important for reproducible MCD difference spectra.

RESULTS

Ultrafast magnetization dynamics measurements, taken by pulsed inductive microwave magnetometery (PIMM), are shown in Figure 1. The responses of three films are shown, for bias fields H_B=20 Oe: undoped $Ni_{81}Fe_{19}$, Gd-doped $Ni_{81}Fe_{19}$, and Tb-doped $Ni_{81}Fe_{19}$, each 50 nm thick with a 2 nm Ta cap. The fast risetime pulse is applied at $t \simeq 0.7$ns.

It can be seen that the Tb-doped sample experiences a much larger damping of magnetization motion than do the undoped or Gd-doped samples. This behavior can be connected with the materials parameter λ through the LL equation (SI units),

$$\frac{d\mathbf{M}}{dt} = -\mu_0 \mid \gamma \mid (\mathbf{M} \times \mathbf{H}) - \frac{\lambda}{M_s^2} (\mathbf{M} \times \mathbf{M} \times \mathbf{H}), \tag{1}$$

where $\mathbf{M}$ is the magnetization, $\mathbf{H}$ is the effective applied field including demagnetizing and anisotropy components, γ is the gyromagnetic ratio, and λ is the relaxation rate in s^{-1}. The second term describes the relaxation of the motion. A time-domain solution can be written valid for small rotation angles and single domain behavior[17]

$$\phi(t) = \phi_0 + \beta_0 e^{-\lambda t/2} \sin(\omega_p t + \varphi) \tag{2}$$

where ϕ_0, β_0, and φ are constants. Fits to this equation are pictured with the PIMM data. We find relaxation rates λ of 0.9 GHz for undoped $Ni_{81}Fe_{19}$, 0.90 for Gd(2%)-doped $Ni_{81}Fe_{19}$, and 4.2 GHz for Tb(2%)-doped $Ni_{81}Fe_{19}$.

XMCD characterization of the local magnetization states on RE dopants is shown in Figure 2. X-ray absorption spectra for Gd and Tb are shown in the top panel; XMCD measurements are shown in the middle panel (dots). The XMCD data have been smoothed

using a polynomial fit with variable window position (lines); the smoothed data, integrated numerically over energy, are shown in the bottom panel.

The nominal XAS peak positions at M_5 and M_4 correspond within ± 0.7 eV to published values for elemental Tb and Gd samples[13, 14, 18]. Main peaks are seen for Gd at 1184.7 eV(M_5), 1213.8 eV(M_4) and Tb at 1238.7 eV(M_5), 1271.7 eV(M_4). Additionally, Gd exhibits a small shoulder on the high energy side of M_5 and a split peak in M_4 consistent with refs[14, 18].

XMCD characteristics are quite different for Gd and Tb. Gd shows a positive and negative peak at M_5 and M_4 respectively. Tb shows a net positive peak at M_5, with a small negative peak on the low energy side, and a small disturbance at M_4 on the threshold of experimental error. Tb observations are consistent with elemental Tb XMCD spectra found by van der Laan et al[13]; here the negative peak on M_5 and small positive and negative peaks at M_4 are roughly 15% and 7% the heights of the large positive peak at M_5.

The bottom panel shows the energy integrals of the two XMCD peaks, following the method in [19] for application of sum rules. A and B are the integrals over M_5 and M_4 XMCD, respectively. Orbital to spin number ratios $< L > / < S >$ obtained at $M_{4,5}$ edges can be determined from the formula[11, 12]

$$\frac{< \hat{L}_z >}{< \hat{S}_z >} = 2\frac{|A| - |B|}{|A| + \frac{3}{2}|B|}\left(1 + \frac{< \hat{T}_z >}{< \hat{S}_z >}\right) \tag{3}$$

where T_z is the magnetic dipole operator. We extract, for Gd, $A = B = 0.027 \pm 0.004$, and for Tb, $A = 0.026 \pm 0.002$, $B = 0.000 \pm 0.002$. Jo et al[21] have published estimates for $< T_z > and < S_z >$ for all lanthanides, excepting Eu, according to atomic calculations, yielding $< T_z/S_z >_{Gd} = -0.009$ and $< T_z/S_z >_{Tb} = -0.08$.

Estimates of orbital to spin number ratios (twice the magnetic moment ratios) are given in Table I. We find $< L_z/S_z >_{Gd} = 0.0 \pm 0.1$, and $< L_z/S_z >_{Tb} = 1.5 \pm 0.3$. These values are in qualitative agreement with Hund's rule estimates. Gd (Z=64, $4f^7$) has $S = 7/2$, $L = 0$ ($L/S = 0$), and Tb (Z=65, $4f^8$) has $S = 3$, $L = 3$ ($L/S = 1$).

DISCUSSION

XMCD measurements show a great difference between the magnetic character of dilute Gd and Tb in $Ni_{81}Fe_{19}$. Gd is found to be pure spin type (S-state) and dilute Tb is found

to have roughly equal parts spin and orbital moment. The approximation of the isolated $4f^{Z-57}$ moment is broadly validated for these two rare-earth dopants in $Ni_{81}Fe_{19}$, although the Tb L/S value is roughly 50% higher than that found through calculation. Alternate handling of the spin sum rule, such as the conventional neglect of the $< T_z >$ term, increases the disagreement. Based on the conclusion of [21], the validity of the spin sum rule is not seriously in question for these two elements, although it may not hold for the lighter lanthanides.

The XMCD measurement verifies an important criterion for an atomistic basis of contributed damping in doped $Ni_{81}Fe_{19}$. It has been proposed that the presence of spin-orbit coupling is essential for the damping of uniform precession by electronic excitations[22, 23] which can ultimately be absorbed by a phonon and dissipated as heat. Rare-earth elements can provide local centers for spin-orbit coupling: the orbital moment of the RE can couple to the Fe, Ni spin system through the RE spin moment. A necessary criterion for this mechanism is the presence of an orbital moment on RE sites which enhance the damping. We have validated its presence in Tb and absence in Gd.

CONCLUSION

We have seen that XMCD characterization of Tb and Gd dopants in $Ni_{81}Fe_{19}$ reveals a large orbital moment fraction on Tb sites, accompanied by a large increase in precessional damping, but zero orbital moment on Gd, with no effect on precessional damping. The results provide support for the idea that spin-orbit coupling, through introduction of local orbital moments, is important for controlled damping from lanthanide dopants.

ACKNOWLEDGEMENTS

We thank Dario Arena and Joe Dvorak (NSLS / U4B) for beamline support and Sasha Bakru for RBS measurements. Research was carried out in part at the National Synchrotron Light Source, Brookhaven National Laboratory, which is supported by the U.S. Department of Energy, Division of Materials Sciences and Division of Chemical Sciences, under Contract No. DE-AC02-98CH10886. We acknowledge the NIST Nanomagnetodynamics Program (606NANB2D0145) for support.

[1] R. Koch, G. Grinstein, G. Keefe, Y. Lu, P. Troulloud, W. Gallagher, and S. Parkin, Physical Review Letters **84**, 5419 (2000).

[2] S. E. Russek, S. Kaka, and M. J. Donahue, Journal of Applied Physics **87**, 7070 (2000).

[3] T. Silva, C. Lee, T. Crawford, and C. Rogers, Journal of Applied Physics **85**, 7849 (1999).

[4] C. Back, R. Allenspach, W. Weber, S. Parkin, D. Weller, E. Garwin, and H. Siegmann, Science **285**, 864 (1999).

[5] W. Bailey, P. Kabos, F. Mancoff, and S. Russek, IEEE Transactions on Magnetics **37**, 1749 (2001).

[6] S. Ingvarsson, L. Ritchie, X. Liu, G. Xiao, J. Slonczewski, P. Trouilloud, and R. Koch, Physical Review B (Condensed Matter and Materials Physics) **66**, 214416 (2002).

[7] S. Reidy, L. Cheng, and W. Bailey, Applied Physics Letters **82**, 1254 (2003).

[8] P.-G. DeGennes, C. Kittel, and A. Portis, Physical Review **116**, 323 (1959).

[9] P. Seiden, Physical Review **133**, A728 (1964).

[10] S. Chikazumi and S. Charap, *Physics of Magnetism* (John Wiley and Sons, 1964).

[11] B. Thole, P. Carra, F. Sette, and G. van der Laan, Physical Review Letters **68**, 1943 (1992).

[12] P. Carra, B. Thole, M. Altarelli, and X. Wang, Physical Review Letters **70**, 694 (1993).

[13] G. van der Laan, E. Arenholz, Z. Hu, A. Bauer, E. Weschke, C. Schussler-Langeheine, E. Navas, A. Muhlig, G. Kaindl, J. Geodkoop, et al., Physical Review B (Condensed Matter) **59**, 8835 (1999).

[14] Z. Hu, K. Starke, G. van der Laan, E. Navas, A. Bauer, E. Weschke, E. Schussler-Langeheine, E. Arenholz, A. Muhlig, G. Kaindl, et al., Physical Review B (Condensed Matter) **59**, 9737 (1999).

[15] V. Chakarian, Y. Idzerda, and C. Chen, Physical Review B (Condensed Matter) **57**, 5312 (1998).

[16] G. Kaindl, G. Kalkowski, W. Brewer, B. Perscheid, and F. Holtzberg, Journal of Applied Physics **55**, 1910 (1984).

[17] T. Crawford, T. Silva, C. Teplin, and C. Rogers, Applied Physics Letters **74**, 3386 (1999).

[18] B. Thole, G. van der Laan, J. Fuggle, G. Sawatzky, R. Karnatak, and J.-M. Esteva, Physical Review B (Condensed Matter) **32**, 5107 (1985).

[19] C. Chen, Y. Idzerda, H.-J. Lin, N. Smith, G. Meigs, E. Chaban, G. Ho, E. Pellegrin, and F. Sette, Physical Review Letters **75**, 152 (1995).

[20] B. Thole, G. van der Laan, and G. Sawatzky, Physical Review Letters **55**, 2086 (1985).

[21] Y. Teramura, A. Tanaka, B. Thole, and T. Jo, Journal of the Physical Society of Japan **65**, 3056 (1996).

[22] V. Korenman and R. Prange, Physical Review B (Solid State) **6**, 2769 (1972).

[23] V. Kamberský, Canadian Journal of Physics **48**, 2906 (1970).

[24] This thickness was found to be optimal for XMCD measurements, as zero cap layer thickness produced Fe and Ni MCD spectra characeristic of oxide, and 50 Å Ta caps provided a large attenuation of the MCD signal.

Figures

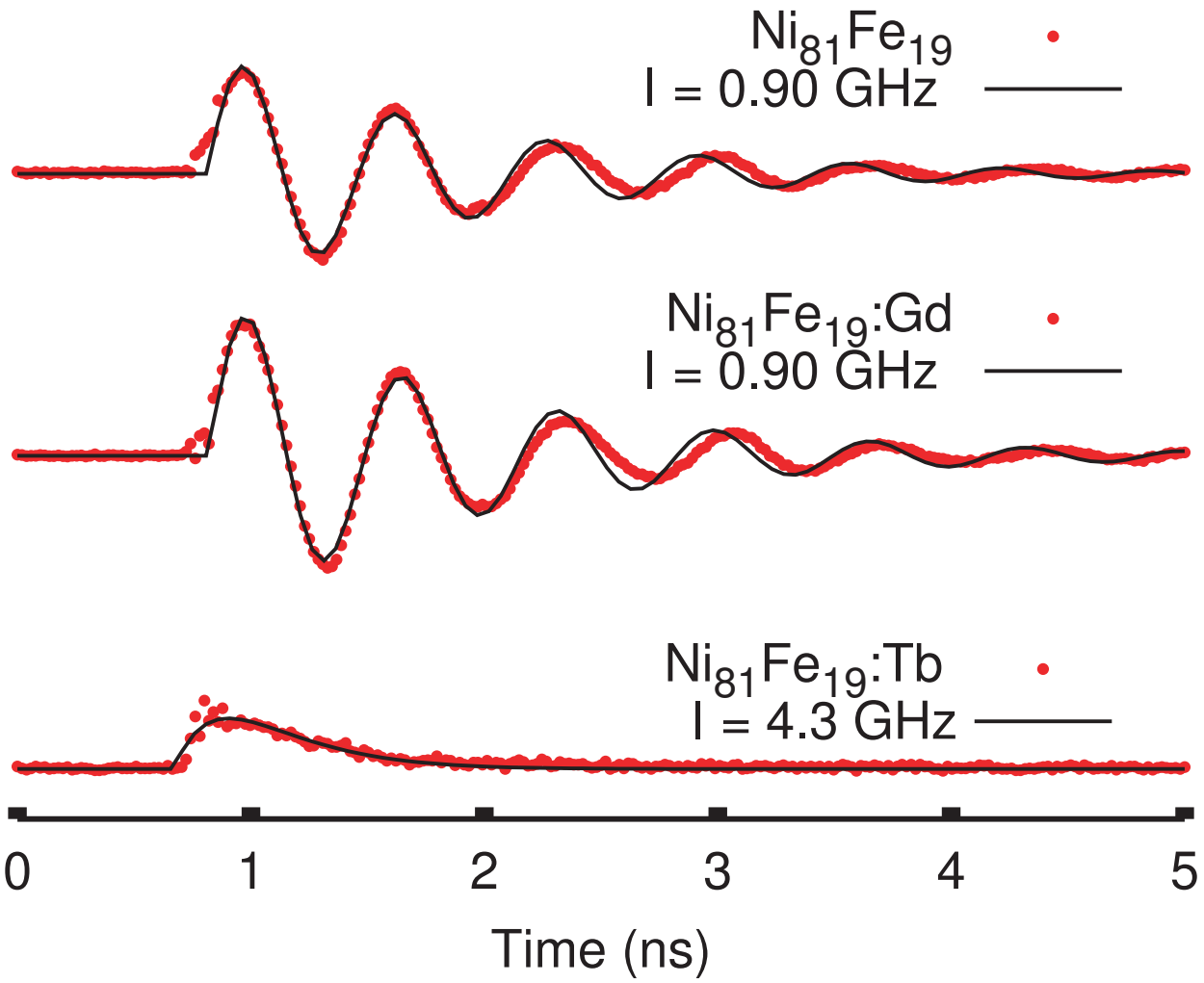

FIG. 1: Inductive measurement of magnetization dynamics for undoped, Gd(2%)-doped, and Tb(2%)-doped $Ni_{81}Fe_{19}$(50nm) thin films, with LL-model fits.

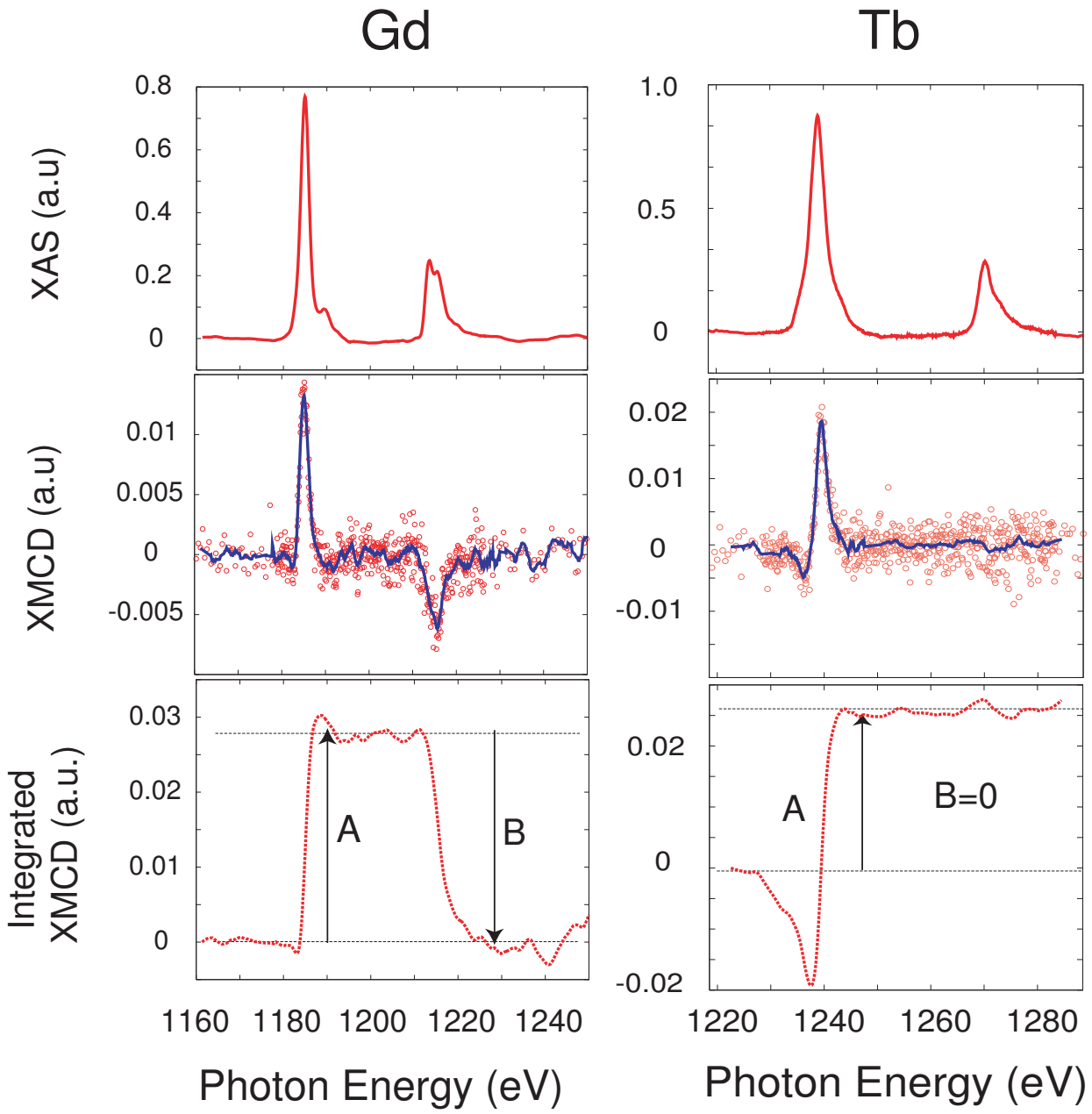

FIG. 2: XMCD characterization of RE dopant magnetism in $Ni_{81}Fe_{19}$:RE(2%), RE=Gd,Tb. *Top:* x-ray absorption spectra (XAS), *middle:* XMCD difference data (circles) with polynomial smoothing fit (lines); *bottom:* energy integral of XMCD spectra. Bottom figures are the integrals of middle figures. The M_5 XMCD integral A and M_4 XMCD integral B are indicated.

Tables

L/S ratio	Tb	Gd
XMCD experiment	1.5±0.3	0.0 ± 0.1
Hund's rule, $4f^{Z-57}$	1	0

TABLE I: Orbital to spin moment ratios L/S on rare-earth dopants RE=(Tb, Gd) in $Ni_{81}Fe_{19}$:RE(2%)(50nm), as measured by XMCD and predicted by Hund's rules. The range of L/S estimate for Tb depends on the spin sum rule used; see text for details.